Published in final edited form as:
J Reprod Immunol. 2011 April ; 89(1): 26–37. doi:10.1016/j.jri.2011.01.018.

Spermatogenetic But Not Immunological Defects in Mice Lacking the τCstF-64 Polyadenylation Protein[1]

Kathy J. Hockert[3], **Kathleen Martincic**[5], **S. M. L. C. Mendis-Handagama**[4], **Lisa Ann Borghesi**[5], **Christine Milcarek**[5], **Brinda Dass**[3,†], and **Clinton C. MacDonald**[2,3]

[3]Department of Cell Biology & Biochemistry, Texas Tech University Health Sciences Center, Lubbock, TX 79430-6540

[4]Department of Comparative Medicine, College of Veterinary Medicine, The University of Tennessee, Knoxville, TN 37996

[5]Department of Molecular Genetics and Biochemistry, University of Pittsburgh School of Medicine, Pittsburgh, PA 15261

Abstract

Alternative polyadenylation controls expression of genes in many tissues including immune cells and male germ cells. The τCstF-64 polyadenylation protein is expressed in both cell types, and we previously showed that *Cstf2t*, the gene encoding τCstF-64 was necessary for spermatogenesis and fertilization. Here we examine consequences of τCstF-64 loss in both germ cells and immune cells. Spermatozoa from *Cstf2t* null mutant *(Cstf2t*$^{-/-}$*)* mice of ages ranging from 60 to 108 days postpartum exhibited severe defects in motility and morphology that were correlated with a decrease in numbers of round spermatids. Spermatozoa in these mice also displayed severe morphological defects at every age, especially in the head and midpiece. In the testicular epithelium, we saw normal numbers of cells in earlier stages of spermatogenesis, but reduced numbers of round spermatids in *Cstf2t*$^{-/-}$ mice. Although Leydig cell numbers were normal, we did observe reduced levels of plasma testosterone in the knockout animals, suggesting that reduced androgen might also be contributing to the *Cstf2t*$^{-/-}$ phenotype. Finally, while τCstF-64 was expressed in a variety of immune cell types in wild type mice, we did not find differences in secreted IgG or IgM or changes in immune cell populations in *Cstf2t*$^{-/-}$ mice, suggesting that τCstF-64 function in immune cells is either redundant or vestigial. Together, these data show that τCstF-64 function is primarily to support spermatogenesis, but only incidentally to support immune cell function.

Keywords

sperm; infertility; oligoasthenoteratozoospermia; fertilization; B cells; immunity

[1]Grant support: Supported by the South Plains Foundation, the TTUHSC School of Medicine, and a National Institutes of Health Grant (HD037109) to C. C. M.

[2]Correspondence and reprint requests: Clinton C. MacDonald, Ph. D., Department of Cell Biology and Biochemistry, Texas Tech University Health Sciences Center, 3601 Fourth Street Texas, Lubbock, TX-79430, USA. Tel: 1-806-743-2700 Ext: 253; Fax: 1-806-743-2990: clint.macdonald@ttuhsc.edu.
[†]Current address: Food & Drug Administration, Center for Veterinary Medicine, Office of New Animal Drug Evaluation, 7500 Standish Place, Rockville MD 20855, USA

1. Introduction

Impairment of spermatogenesis is one of the most common forms of human infertility (Hirsh 2003), although the physiological basis is often not defined (Isidori et al. 2005). The complex genetic control of spermatogenesis (Grootegoed et al. 2000) has led to the conclusion that a significant number of these infertilities are due to autosomal recessive genes, including many involved in transcriptional and post-transcriptional gene expression (Bhasin et al. 2000). One protein that is important for post-transcriptional control of germ cell mRNA processing is τCstF-64 (official symbol CSTF2T), the germ cell-expressed paralog of the CstF-64 (official symbol CSTF2) polyadenylation protein (Dass et al. 2002; Dass et al. 2001; Wallace et al. 1999). In male mice, *Cstf2t* (the gene encoding τCstF-64) is expressed during meiosis when the X-linked *Cstf2* (which encodes CstF-64) is not expressed due to meiotic sex chromosome inactivation (MSCI (Handel 2004; Turner 2007; Zamudio et al. 2008)). Therefore, *Cstf2t* falls into the class of retroposons that are expressed in meiosis to compensate for loss of expression of X-linked genes (Khil et al. 2004; Wang 2004). However, τCstF-64 is not expressed exclusively in male germ cells, but has been observed in thymus (Beyer et al. 1997; Wallace et al. 2004), brain (Wallace et al. 1999; Wallace et al. 2004), spleen, and liver (Wallace et al. 2004), while its mRNA is expressed in all tissues (Huber et al. 2005). This suggests that τCstF-64 might have both reproductive and non-reproductive functions.

Targeted deletion of *Cstf2t* resulted in male infertility due to multiple defects in spermatogenesis (Dass et al. 2007). Those defects included lesions in secondary spermatocytes, cumulative histological abnormalities in step 10 and later elongating spermatids, and a failure to release mature spermatids into the lumen of the seminiferous tubules. Epididymal sperm from mice with a null mutation in the *Cstf2t* gene, *Cstf2t*$^{tm1Ccma/tm1Ccma}$ mice (herein, *Cstf2t*$^{-/-}$ mice) showed considerable debris, unusual round cells (Tardif et al. 2010), and significantly fewer spermatozoa than in wild type mice, a condition that resembled oligoasthenoteratozoospermia in infertile men (Hirsh 2003; Isidori et al. 2005). Furthermore, the *Cstf2t*^{tm1Ccma} allele exhibited variable expressivity, *i.e.* individual postmeiotic germ cells displayed different degrees of defects ranging from a block to differentiation beyond round spermatid stages to morphologically incomplete, but motile spermatozoa (Dass et al. 2007). These spermatozoa were not capable of fertilizing eggs in vitro, suggesting that genes required for function during interaction of motile spermatozoa with eggs are incorrectly expressed (Tardif et al. 2010). Together, these defects suggested that a variety of developmental, structural and functional genes were affected in the *Cstf2t*$^{-/-}$ mice, a conclusion that is supported by the large number of mRNAs whose expression was altered (Dass et al. 2007). Our first goal in this report was to characterize more completely the defects in the *Cstf2t*$^{-/-}$ spermatozoa. Further, since developmental abnormalities can vary with age, our second goal was to determine whether mice of different ages displayed different defects in their spermatozoa.

τCstF-64 expression is not restricted to male germ cells, however. We detected the τCstF-64 protein in brain (Wallace et al. 1999), spleen, and thymus (Wallace et al. 2004), and the mRNA was expressed in all tissues (Huber et al. 2005). These data suggested possible roles for τCstF-64 in tissues other than testis. We have not observed overt differences in behavior of the *Cstf2t*$^{-/-}$ mice; thus, we have not pursued a neurological phenotype. However, immunological differences in these mice might be subtle. CstF-64 has been shown to regulate the switch in immunoglobulins from a membrane-bound to a secreted form (Takagaki et al. 1996). Therefore, our third goal was to examine possible changes in immune cell function in *Cstf2t*$^{-/-}$ mice.

In this report, we show that the infertility we reported previously (Dass et al. 2007; Tardif et al. 2010) was correlated with severe defects in sperm cell function in adult mice of every age. Those spermatozoa that were present were mostly microcephalic with misshapen heads and thin or short midpieces. Defects in spermatozoa correlated with reduced seminiferous tubule diameters due to loss of round spermatids and disrupted spermiation. We observed reduced numbers of round spermatids in *Cstf2t*$^{-/-}$ mice, but not of earlier germ cell types. We also observed reduced testosterone that was not correlated with a reduction in numbers of Leydig cells. τCstF-64 is expressed in a number of immune cell types including splenocytes and bone marrow cells, and is in complex with other CstF proteins in mouse memory lymphoma and hybrid myeloma cell lines, suggesting it participates in polyadenylation in these cells. However, we saw no differences in immune cell function as determined by amounts of plasma IgG or IgM, or populations of granulocytes, macrophages, B cells, natural killer cells or T cells in the spleen or bone marrow. We did, however, observe parallel increases in CstF-64 and τCstF-64 in CstF complexes upon lipopolysaccharide (LPS) stimulation of spleen cells. This suggests that τCstF-64 functions in parallel to CstF-64 in stimulated immune cells in a manner that differs from its unique and necessary function in male germ cells.

2. Materials and methods

2.1 Animal Studies

Animal experiments were performed at Texas Tech University Health Sciences Center or University of Tennessee, Knoxville in accordance with protocols that were approved by each institution ’s Institutional Animal Care and Use Committee, and following NIH guidelines. For all other studies, samples were prepared at Texas Tech University Health Sciences Center and shipped to the respective institutions. Deletion of the entire *Cstf2t* coding region from chromosome 19 (*Cstf2t*^{tm1Ccma}), breeding, and genotyping were described previously (Dass et al. 2007). *Cstf2t*^{tm1Ccma} mice used in these studies were of mixed C57BL/6–129SvEv background. For all studies, littermates or age-matched mice from the same generation were used when possible to minimize variation.

Male mice were euthanized at 43, 60, 85 and 108 days postpartum (dpp) and the intact body was weighed, dissected, and weights obtained for each testis, epididymis and seminal vesicle. Statistical comparisons of the weights (ANOVA) were performed using Graph Pad InStat software (San Diego, CA).

2.2 Computer Assisted Sperm Analysis (CASA)

Cauda epididymides from 43, 60, 85 or 108 dpp *Cstf2t*$^{+/+}$, *Cstf2t*$^{+/-}$, and *Cstf2t*$^{-/-}$ mice were minced at 37°C in modified Tyrode’s medium, 5% CO_2, pH 7.4, supplemented with 1.8 mM $CaCl_2$, 0.4% BSA and 0.5 mM pyruvate prior to use, and incubated for 10 minutes at 37°C, 5% CO_2 to release spermatozoa. Cell concentration was adjusted to 8 million/ml and CASA performed using the Hamilton Thorne Biosciences Ceros system (Beverly, MA) on an Olympus CX-41 microscope fitted with a CCD camera and Minitherm slide warmer (Quill et al. 2003). Sperm cell tracks were captured in an 80 μm chamber at 60 Hz. Ten arbitrary and independent fields were captured for at least four male mice of each age and genotype, analyzing 60–100 spermatozoa per field. Video of the spermatozoa was captured using the same system.

2.3 Sperm Morphology Analysis

Approximately 15 μL of the sperm in m-Tyrode’s medium per slide was used to prepare each smear. Each slide was allowed to air dry for approximately 10 to 15 minutes before staining with the STAT II Andrology Staining Kit (Mid-Atlantic Diagnostics, Inc., Mt.

Laurel, NJ) followed by a distilled water wash and air drying. The slides were then viewed on the Olympus BX-60 microscope at 40×. Samples were examined and scored for the following anomalies: heads (misshapen head, microcephalous, macrocephalous, multiple heads, head misplaced with respect to the tail), midpieces (cytoplasmic droplet, thin midpiece, folded at or just following the midpiece), and tails (absent, short, irregular, coiled, multiple). Note that, due to the decreased number of recognizable spermatozoa in the *Cstf2t*$^{-/-}$ mice, a larger number of fields were examined to count the same number of spermatozoa. Common combination categories were also recorded (Combination 1, misshapen and variably microcephalous head; Combination 2, misshapen, variably microcephalous head and thin or completely indistinguishable midpiece).

2.4 Histology

2.4.1 Fixation and Processing of Testicular Tissue—Mice were euthanized via inhalation of isoflurane (Abbott Laboratories, Deerpark, IL) and one testis was removed, dissected free from the epididymis, weighed (fresh weight of the testis) and specific gravity was determined by flotation method (Mendis-Handagama and Ewing 1990). This testis was used for the determination of LH-stimulated testicular testosterone secretory capacity in vitro as described below. A sample of blood was also collected by cardiocentesis at this time to determine the plasma testosterone levels. The intact testis in each mouse was fixed in-situ by whole body perfusion technique (Ariyaratne and Mendis-Handagama 2000; Mendis-Handagama et al. 1998; Mendis-Handagama et al. 1988) using 5% glutaraldehyde in cacodylate buffer. The fixed testis was removed, weighed (fixed testis weight) and specific gravity was determined. Then the testis was cut in to approximately 2 mm × 3 mm blocks, post-fixed in a mixture of osmium tetroxide and potassium ferrocyanide, dehydrated in a series of graded ethanols and embedded in epon-araldyte. Separate tissue blocks were processed in a similar manner to determine the shrinkage factor as described previously (Mendis-Handagama and Ewing 1990).

2.4.2 Stereology—Cell numbers per Testis: One micrometer thick serial sect ions were cut from epon-araldyte-embedded tissue blocks using a LKB Ultramicrotome V (Pharmacia LKB, Piscataway, NJ) and glass knives. From the serial sections, two sections that were four sections apart (i. e., the 1st and 5th sections) were collected and mounted on a glass slide close to each other, stained with methylene blue and azure, then mounted under cover slips with Permount (Fisher Scientific, Fair Lawn, NJ). Leydig, Sertoli and germ cells were identified by their characteristic morphology and their numbers per testis were determined using the dissector principle as described previously (Ariyaratne and Mendis-Handagama 2000; Mendis-Handagama and Ewing 1990; Sterio 1984). Twenty to 30 fields per block and 10 blocks per mouse were scored; there were 7–8 mice per experimental group.

Seminiferous Tubule Diameter and Length: Seminiferous tubule diameters (D) were measured using a stage and an ocular micrometer (Mendis-Handagama et al. 2010) under ×40 objective and ×10 ocular (8–10 seminiferous tubules/section, four sections/mouse, 7–8 mice/experimental group). The length of each seminiferous tubule was determined as previously described (Mendis-Handagama et al. 2010).

Volume of Testicular Components per Testis: Volume density (defined as volume of component per unit volume of testis) of testicular components (seminiferous tubules, testis interstitium, lymphatic space, Leydig cells, macrophages and blood vessels) was determined by the point counting method as described (Ariyaratne and Mendis-Handagama 2000; Mendis-Handagama et al. 1998). The test system contained a square lattice grid with 121 test points that was fitted to the eyepiece of the light microscope (Olmpus BH-2, Olympus, Tokyo, Japan).

2.5 Hormones

2.5.1 LH-Stimulated testicular testosterone secretory capacity in vitro—Each mouse testis was decapsulated, teased, and incubated in 2 ml of Krebs-Ringer bicarbonate buffer (pH 7.4) supplemented with 0.004 g/ml glucose and LH (ovine LH, 100 ng/ml; NIDDK Hormone Distribution Program, Torrance, CA) as previously described (Mendis-Handagama et al. 2010; Mendis-Handagama et al. 1998; Mendis-Handagama et al. 1990). Before addition of glucose, the incubation medium was saturated with air for 10 minutes. Incubations were performed in 20-ml scintillation vials at 34°C in an oscillating water bath (90 oscillations/min). At the end of 3 hours, the incubation medium was collected and centrifuged at 3000×g for 10 min, and the supernatant was separated and stored at −80°C until further analysis.

2.5.2 Radioimmunoassay (RIA) for Testosterone—Testosterone concentrations in the plasma and in vitro incubation media were determined by using commercially available RIA kits (Coat-A-Count; DPC, Los Angeles, CA). The sensitivity of this assay was 0.14 nM. The intra-assay coefficient of variation was less than 8%. The cross reactivity of the antibody used was 2.8% for dehydrotestosterone, 0.5% for androstenedione, and less than 0.02% for other steroids.

2.6 Tissue Culture and Primary Cells

A20 mouse memory lymphoma cells were cultured as previously described (Edwalds-Gilbert and Milcarek 1995).

2.7 Extraction of Splenic Bone Marrow Cells

Spleens and hind legs from male C57B6 or *Cstf2t*$^{-/-}$ mice were removed and then held on ice overnight or harvested immediately. Splenic cells were released by grinding the spleen between the frosted ends of two glass slides. Cells were then diluted in staining media (Dulbecco's PBS without Ca^{++} or Mg^{++}, supplemented with 3% FCS, 1mM EDTA pH 7.5, and 0.02% sodium azide) and centrifuged at 1200 rpm for 10 min. Red blood cells were lysed by diluting in hypotonic medium and then immediately equilibrated by the addition of 1/10 vol of 10× PBS. Cells were centrifuged, diluted in staining medium and filtered through a 50 μm mesh, and adjusted to 3×10^7 cells per ml. Cells from the bone marrow were flushed with cold staining medium, centrifuged, then treated with ACK lysing buffer (BioWhittaker/Cambex, East Rutherford, NJ) for 2 min at room temp. Cells were diluted, centrifuged, and filtered as described above and adjusted to the same concentration.

2.8 Culturing Splenic Cells With or Without LPS

Splenic cells were plated in Dulbecco's modified Eagle's medium (Invitrogen) at 8×10^6 cells/well in a 2 ml volume in 6 well plates with one-third of the wells receiving 20 μg/ml lipopolysaccharide (LPS, 0111:B4, Sigma, St. Louis, MO) and cultured in a 5% CO_2 37°C incubator or left on ice for 72 hours.

2.9 Flow Cytometry

Approximately 10^6 cells were treated as follows. All steps were performed on ice. For surface staining, cells were blocked with 2.4G2, anti Fc receptor, in 5% FCS and 2.5% BSA in PBS for 10 min, then incubated with surface antibodies: Gr-1-PE, CD11b-Cy7PE, CD19-Cy5PE, B220-PE or B220-APC, IgM-APCSyndecan-biotin followed by streptavidin-Cy5PE, NK1.1-PEor CD3-Cy5PE for 20 min, washed twice, then incubated in 2% paraformaldehyde for 10 min. All surface antibodies were obtained from eBioscience, San Diego, CA. For internuclear staining, after paraformaldehyde fixation, cells were washed once with staining media, then resuspended in ice cold 95% ethanol/5% PBS, added

dropwise while gently mixing cells, incubated for 10 min, washed with PBS, then incubated with 2.4G2 block as above. Cells blocked with the 3A7 or 6A9 monoclonal antibodies (see below) were incubated with 15 μg purified unlabelled monoclonal antibodies for 30 min before receiving 25 ng fluorescein-5-isothiocyanate conjugated monoclonal antibodies, which were labeled according to the manufacturer's recommendations (Molecular Probes/ Invitrogen, Eugene, OR). Cells were labeled for 30 min, then washed thrice, and fixed with 2% paraformaldehyde again. Cells were diluted into staining media and run on the BD LSRII (Becton-Dickinson, Franklin Lakes, NJ) and analyzed with FlowJo (TreeStar, Inc., Ashland, OR) using Microsoft Excel software.

2.10 Protein Samples, Immunoprecipitation and Immunoblotting

Nuclear extracts were prepared as described previously (Edwalds-Gilbert and Milcarek 1995). Lysates were prepared as follows: 3×10^6 cells were lysed in 60 μl of a buffer containing 1% Triton-100, 0.1% SDS, 50 mM Tris-HCl, pH 8, 150mM NaCl plus protease inhibitors (Calbiochem, Gibbstown, NJ) and incubated 30 min on ice, then clarified before adding SDS-PAGE sample buffer and boiling. For whole cell lysates, the same number of cells were resuspended in 30 μl of PBS to which was added 30 μl of 124 mM Tris-HCl, pH 6.8, 200 mM DTT, 4% SDS, 20% glycerol. Samples were immediately boiled for 5 min. Western blots were performed as previously described (Edwalds-Gilbert and Milcarek 1995) and probed with the 3A7 (anti-CstF-64) or 6A9 (anti-τCstF-64) monoclonal antibodies (Wallace et al. 1999), R5180, a rabbit antibody that recognizes the COOH-terminal peptide conserved between human and mouse CstF-64 and τCstF-64, or rabbit anti-CstF-77 that was raised against the VLKDEVDRKPEYPKPDTQQMIPFQP peptide. Signals were visualized chemiluminescently with Western Lightning (PerkinElmer, Boston, MA).

Immunoprecipitations were performed in the following manner: 150 μg of nuclear extract or 1.5×10^7 cells washed and lysed in lysis buffer (50mM Tris-HCl, pH 7.9, 300 mM NaCl, 1 mM EDTA, 1 mM DTT, 1% NP40, protease inhibitors) was precleared with anti-mouse IgG plus Protein G, then incubated with the 2C1 (anti-CstF-50; Takagaki et al. 1990), 3A7, or OKT8 (CD8, ATCC, Manassas, VA) monoclonal antibodies for 1 hour on ice, washed four times with lysis buffer, then boiled in SDS-PAGE sample buffer and loaded on the EZ-Run 10% gel system (Fisher BioReagents, Pittsburgh, PA). To enhance signal, four times as much protein was loaded on blots probed with 6A9 as with 3A7 and the signal was further enhanced using the Pierce Qentix Western Blot Signal Enhancer before blocking. Blots were visualized with Supersignal Femto substrate (Pierce, Rockford, IL).

2.11 Capture ELISA

Capture ELISAs were performed on blood obtained by cardiac puncture from 43, 60, 85 or 108 dpp male mice as follows. 96 well plates were coated with either 40 μg/ml anti-mouse IgM F(ab')2 (Cappel/MP, Solon, OH), or 4 μg/ml anti-mouse IgG (Sigma) overnight at 4°C. Plates were washed three times with PBS, blocked with 10% BSA/PBS for 2 hours at room temperature, and washed again. Wells were then filled with either 50 μl of a standard curve, 1 to 0.008 μg/ml of pure myeloma protein IgM (Cappel) or purified immunoglobulin IgG (Sigma, St, Louis, MO), or 50 μl of mouse sera diluted 1:500 for IgM or 1:1000 for IgG, incubated for 1 hour at 37°C, washed, and developed with TM Blue (KPL, Gaithersburg, MD). The TM Blue reaction was stopped with 1.0 NH_2SO_4 and absorbance at 450 nm determined on a MRX Revelations plate reader. Points represent individual mice, which were then averaged and plotted.

3. Results

3.1 Spermatozoa from *Cstf2t*$^{-/-}$ Males Show a Large Number of Motility Defects at Every Age

Computer-assisted sperm analysis (CASA) examines a number of parameters that correlate with viability and fertility in sperm samples (Verstegen et al. 2002). Previously, we described results from CASA of cauda epididymal spermatozoa from 110 dpp *Cstf2t*$^{+/+}$, *Cstf2t*$^{+/-}$, and *Cstf2t*$^{-/-}$ mice (Dass et al. 2007). In that study, we noted that several parameters of sperm function such as motility and progressivity were significantly decreased in *Cstf2t*$^{-/-}$ than in wild type or heterozygous mice, although other parameters (amplitude of lateral head displacement, ALH, curvilinear velocity, VCL, and linear velocity) were not significantly different. However, as these results were from a relatively small group of mice, and fertility and spermatozoa morphology can change with age past the first round of spermatogenesis, we chose to study whether the CASA parameters were valid for larger populations of mice at a variety of ages. Caudal epididymal spermatozoa from *Cstf2t*$^{+/+}$, *Cstf2t*$^{+/-}$, and *Cstf2t*$^{-/-}$ mice at 43, 60, 85, and 108 dpp were analyzed by CASA. Sperm cell tracks within ten arbitrary and independent fields were captured for four male mice of each genotype, analyzing 60–100 spermatozoa per field.

In examining the CASA values for 43 dpp mice, we saw large variations in parameters such as motility and progressivity in all three genotypes; these variations did not pass tests for normality (Supplemental Table 1). This suggested that mice at this age were still undergoing significant spermatogenic development concomitant with the first wave of spermatogenesis. Thus, we did not evaluate 43 dpp mice further for this study.

Comparing wild type mice at 60, 85, and 108 dpp showed that the percentage of motile spermatozoa in these mice did not differ at any age, averaging 82.7% motility (Fig. 1A and Supplemental Table 1). Further, sperm motility in *Cstf2t*$^{+/-}$ mice did not differ significantly from wild type mice (Fig. 1A). Progressivity did not differ among wild type or heterozygotic mice (Fig. 1B). Similarly, other CASA parameters (VAP, VSL, VCL, ALH, BCF, STR, and LIN) did not differ between *Cstf2t*$^{+/+}$ and *Cstf2t*$^{+/-}$ mice at any age (Supplemental Table 1), suggesting that there are few differences in sperm parameters in mice between 60 and 108 dpp as measured by CASA. These data also agree with our previous assessment that mice heterozygous for *Cstf2t* showed no evidence of reduction in sperm function (Dass et al. 2007; Tardif et al. 2010).

However, sperm motility (Fig. 1A) and progressivity (Fig. 1B) of *Cstf2t*$^{-/-}$ mice of all ages are greatly reduced from wild type and heterozygous values. This finding agrees with our earlier results comparing these parameters in 110 dpp mice (Dass et al. 2007). Several other parameters relating to velocity, linearity and head displacement (VAP, VSL, VCL, and ALH) also differed, whereas parameters relating to beat frequency and linearity (BCF, STR, and LIN) did not differ significantly between wild type, heterozygous and *Cstf2t*$^{-/-}$ mice. We interpret these data to mean that, of the small number of motile spermatozoa detected in the *Cstf2t*$^{-/-}$ mice, only a few display motility characteristics comparable to the wild type or heterozygous mice.

3.2 Spermatozoa in *Cstf2t*$^{-/-}$ Mice Are Grossly Abnormal

Because the CASA data implied that many of the spermatozoa in *Cstf2t*$^{-/-}$ mice were functionally defective, we chose to examine their morphological characteristics. Cauda epididymal contents were examined microscopically, and one hundred spermatozoa from each age and genotype group were scored for defects in heads, midpieces and tails as described in Materials and Methods. In examining the numbers of morphologically normal spermatozoa, we saw no differences between wild type and heterozygous mice at any age

(Fig. 2A). Both showed a majority of normal heads, midpieces and tails, with a minority of misshaped heads, bent tails, and other defects (Supplemental Table 2). By contrast, *Cstf2t*$^{-/-}$ mouse spermatozoa at all three ages were grossly abnormal (Fig. 2A). Specifically, two combinations of defects were most often observed: Combination 1, which was manifested as a misshapen and variably microcephalous head (Fig. 2B); and Combination #2, which was like Combination 1 but with additionally thin or completely indistinguishable midpieces (Fig. 2C). These particular combinations were never observed in the wild type or heterozygous animals. However, together these defects accounted for as much as 87% of the spermatozoa observed in *Cstf2t*$^{-/-}$ mice. This suggests that some of the motility defects observed by CASA in the *Cstf2t*$^{-/-}$ mice (Fig. 1) are due to these readily observed structural defects.

3.3 Fewer Round Spermatids Contribute to Decreased Seminiferous Tubule Lumen Size

Since spermatozoa were so abnormal in structure and function, we decided to survey the *Cstf2t*$^{-/-}$ mouse testes for concomitant developmental and structural defects that would contribute to the abnormal spermatozoa. As in our previous study (Dass et al. 2007), we saw no differences in animal weight for any of the genotypes (Fig. 3A). Also as in that study, we saw no significant differences between testis weights in wild type or *Cstf2t*$^{-/-}$ mice (Fig. 3B, bars WT and KO). Unlike that study, here we saw a small but statistically significant difference in testis weights between *Cstf2t*$^{+/-}$ and *Cstf2t*$^{-/-}$ mice (bars HET and KO, $P<0.01$). These and subsequent differences (see below) suggest that a reduced number of copies of the *Cstf2t* gene in heterozygous mice can result in small differences in testis morphology, a phenomenon known as overdominance (Parsons and Bodmer 1961).

The numbers of Leydig cells per testis are identical in *Cstf2t*$^{+/+}$, *Cstf2t*$^{+/-}$, and *Cstf2t*$^{-/-}$ mice (Fig. 3C, bars 1–3). This is expected, since the τCstF-64 protein is expressed exclusively in germ cells, and should not have any direct effects in Leydig cells. Similarly, the numbers of Sertoli cells are not significantly different between *Cstf2t*$^{+/+}$ and *Cstf2t*$^{-/-}$ mice (Fig. 3C, bars 4 and 6), where τCstF-64 is also not expressed. There is a difference between *Cstf2t*$^{+/+}$ and *Cstf2t*$^{+/-}$ mice (bars 4 and 5, $P<0.05$), which might be part of the same overdominance phenomenon seen in testis weights (Fig. 3B). The lack of differences in numbers of somatic cell components is correlated with lack of differences in volumes for the same cell types (Fig. 4E).

Our earlier study identified subtle lesions in secondary spermatocytes and more apparent lesions beginning in step-10 spermatids and subsequent stages (Dass et al. 2007). Notably, spermiation is defective such that step-16 elongating spermatids are not released properly into the seminiferous tubule lumen. Therefore, it is not surprising that we see the most profound differences in late stage germ cells. Numbers of spermatogonia, primary, and secondary spermatocytes do not differ significantly between wild type and *Cstf2t*$^{-/-}$ mice (Fig. 3D, bars 1 and 3, 4 and 6, and 7 and 9). The numbers of primary and secondary spermatocytes seem to differ slightly between *Cstf2t*$^{+/-}$ and *Cstf2t*$^{-/-}$ mice (Fig. 3D, bars 5 and 6, $P < 0.05$ and 8 and 9, $P < 0.01$), possibly reflecting the overdominance phenomenon.

More significantly, numbers of round spermatids differ between wild type, heterozygotic and *Cstf2t*$^{-/-}$ mice (bars 10–12); *Cstf2t*$^{-/-}$ mice having 27% fewer round spermatids than wild type mice. This result correlates with our earlier finding that late stage spermatocytes were most highly affected in the *Cstf2t*$^{-/-}$ mice (Dass et al. 2007). The reduced number of round spermatids in *Cstf2t*$^{-/-}$ mice probably contributes to the reduced seminiferous tubule diameter (Fig. 4A) and volume (Fig. 4C) and the reduced seminiferous tubule lumen volume (Fig. 4D).

3.4 Plasma and Luteinizing Hormone-Stimulated Testosterone Levels are Lowest in *Cstf2t*$^{-/-}$ Mice

Figure 5 shows plasma and LH-stimulated testicular testosterone levels of wild type, heterozygous, and *Cstf2t*$^{-/-}$ mice. Plasma testosterone of *Cstf2t*$^{-/-}$ male mice (Fig. 5A) was less than one-quarter that of wild type mice ($P = 0.0245$), suggesting the possibility of androgen deficiency in these mice. LH-stimulated testicular testosterone in *Cstf2t*$^{-/-}$ mice (Fig. 5B) was also significantly lower than wild type ($P < 0.05$). This suggests that diminished intratesticular testosterone secretory capacity might occur in *Cstf2t*$^{-/-}$ mice.

3.5 Both CstF-64 and τCstF-64 are Expressed in Mouse B Cells

Initial western analyses showed that τCstF-64 protein was expressed in brain, spleen and thymus (Wallace et al. 2004) as well as male germ cells; the mRNA has an even wider distribution than the protein (Huber et al. 2005). Since CstF-64 is involved in control of gene expression in lymphoid cells (Martincic et al. 1998; Shell et al. 2005; Takagaki et al. 1996) we wanted to determine whether τCstF-64 was expressed in cells in the lymphoid line, and whether any immunological abnormalities were detectable in the *Cstf2t*$^{-/-}$ mice.

First, we looked at bone marrow and spleen to determine if CstF-64 and τCstF-64 were expressed in wild -type and *Cstf2t*$^{-/-}$ mice using flow cytometric analyses with directly fluorescently tagged (FITC) antibodies (3A7 and 6A9) which recognize CstF-64 and τCstF-64 respectively, run in separate reactions. We determined the mean fluorescent intensity (MFI) with the antibodies by subtracting the MFI obtained with parallel samples that had previously been blocked with an excess of the same unlabeled antibodies (see Materials and Methods), thereby eliminating possible non-specific reactivity. The MFIs indicate that CstF-64 is expressed in both spleen and bone marrow in wild type mice (Fig. 6A). In the *Cstf2t*$^{-/-}$ mice, the expression of CstF-64 was increased in bone marrow by about 30% ($P = 0.011$). This increase may be a physiological compensation for the loss of τCstF-64 protein. This differs from what we observed previously in testes (Dass et al. 2007) and in spleen cells where we observed no such compensation (Fig. 6A).

Meanwhile, τCstF-64 was seen in both spleen and bone marrow samples from wild type mice. The levels of MFI with the 6A9 antibody were significantly decreased in the *Cstf2t*$^{-/-}$ mice in spleen and bone marrow, as would be expected in mice lacking τCstF-64.

The populations of the various lymphoid cells in the wild type and τCstF-64 knockout mice were determined using antibodies against a panel of lymphoid markers and flow cytometric analyses. The percentage of marker positive cells between wild-type and *Cstf2t*$^{-/-}$ mice did not differ significantly in either bone marrow or spleen samples from at least three mice (Table 1). The markers used for quantification were: Gr-1 for granulocytes, CD11b and NK1.1 for myeloid and NK cells, CD19 and IgM^{+} for B cells, syndecan-1 for plasma cells, B220 for leukocytes, and CD3 for T cells. We therefore conclude that gross differentiation of the lymphoid lineage cells, especially B cells, was unaffected by deletion of τCstF-64 even though it was expressed in bone marrow, where lymphoid progenitors arise. We note, however, that subtle changes in differentiation profiles might escape our means of detection.

Next, we isolated CD19^{+} B cells from mouse spleen and cultured them with LPS for 72 hours or left them at 4°C for the same period of time. LPS induces B cell growth and differentiation into plasma cells that subsequently secrete antibody. As shown in Figure 6B, LPS treatment induced both CstF-64 and τCstF-64 significantly above the 4°C control. Thus both forms of CstF-64 are induced in the differentiation of splenic B cells toward antibody secretion, indicating that the τCstF-64 protein may play a role in Ig production.

For τCstF-64 to play a functional role in mouse B cells, it must participate in polyadenylation as a component of the CstF complex. As shown in Figure 6C an antibody to CstF-50 precipitated CstF-64 both before and after LPS stimulation (Fig. 6C, lanes 4, 5 top panel), demonstrating that those two proteins are in a complex in splenic B cells. An increase in precipitable material is seen following LPS stimulation (lane 5). Similarly, τCstF-64 was detected in immunoprecipitated complexes with CstF-50 both before and after LPS stimulation (lanes 4 and 5, middle) with little remaining in the supernatant (lanes 6 and 7, middle). This suggests that a portion of the active CstF complexes in these cells has τCstF-64 as a component; τCstF-64 therefore likely participates in polyadenylation in these cells. It also appears that a larger fraction of the CstF-64 was precipitated than CstF-64, since there was less in the supernatant. CstF-77, the third member of the CstF complex, was similarly increased after LPS (lanes 4 and 5, bottom). In mouse B and plasma cell lines, we also observed τCstF-64 associated with CstF-50 in a complex (data not shown), which would indicate that it functions there as well in the cleavage and polyadenylation of mRNAs.

3.6 Loss of τCstF-64 Does Not Affect Development of Immune Cells

Since CstF-64 has been shown to have effects on the ratio of membrane-bound to secreted immunoglobulins (Takagaki et al. 1996), we hypothesized that if τCstF-64 were involved in this switch, *Cstf2t*$^{-/-}$ mice should have altered amounts of secretory IgG and IgM. Therefore, we measured secreted IgG and IgM in the blood from wild type, heterozygote, and knockout mice using capture ELISA (Fig. 7). We observed no significant differences in amounts of IgM in the sera of any of these mice (Fig. 7A), suggesting that τCstF-64 does not play a critical role in regulation of immunoglobulin mRNA 3’ end processing in mice.

4. Discussion

Polyadenylation is directly involved in transcription and transcriptional termination (Buratowski 2005; Moore and Proudfoot 2009), and is thus essential for gene expression. Furthermore, polyadenylation plays critical roles in mRNA transport from the nucleus, translation, stability, and localization (Keene 2010; Licatalosi and Darnell 2010), making it important for post-transcriptional regulation. Most of the physiological roles of polyadenylation are due to tissue-specific alternative polyadenylation, resulting in mRNAs that encode different proteins or have other altered properties (Lutz 2008). In a few cases tissue-specific factors have been discovered that control polyadenylation site choice; in other cases core members of the basal polyadenylation machinery are increased, decreased, modified, or replaced by variant forms to control site choice (MacDonald and McMahon 2010). τCstF-64 is an example of one of the latter mechanisms: in germ cells, τCstF-64 is a variant of the CstF-64 protein that is expressed during meiosis and subsequent haploid differentiation when CstF-64 is absent (Dass et al. 2002; Dass et al. 2001; Liu et al. 2007). Targeted deletion of *Cstf2t* in mice demonstrated that τCstF-64 was necessary for normal spermatogenesis and fertilization (Dass et al. 2007; Tardif et al. 2010). Here, we showed that the defects caused by the absence of τCstF-64 resulted in severe defects in sperm motility and morphology in mice ranging in ages from 60 to 108 dpp (Figs. 1 and 2). These defects correlated most strongly with decreased seminiferous tubule diameters due to a significant reduction in numbers of round spermatids (Fig. 3 and 4), most likely due to failure of spermiation. We also showed that the defects do not extend to the immune system: while τCstF-64 is expressed widely in immune cells, we saw no changes in any of the cell types we examined in the *Cstf2t*$^{-/-}$ animals (Fig. 6).

Several interesting phenomena are illuminated by these data. In some of the parameters measured (testis weight, testis/body weight ratio, somatic cell numbers, numbers of secondary spermatocytes), we saw evidence that the heterozygous animals had slightly

greater values than either of the homozygous groups. This is an example of the genetic phenomenon of overdominance. While it is hard to imagine a mechanism by which heterozygosity for *Cstf2t*^{tm1Ccma} would result in a physiological advantage, it does lead to the interesting possibility that *Cstf2t* mutants are maintained in a population by heterozygous advantage, despite the disadvantage to the population of an infertility phenotype. This would explain, for example, the persistence of some infertility alleles in human populations, even though one might otherwise expect them to be eliminated quickly due to the infertile phenotype.

The first hypothesis we wanted to test was whether the defects in spermatogenesis we saw in the *Cstf2t*$^{-/-}$ mice became more severe in older mice. There have been reports in azoospermic rodents of age-related increases in the severity of the defect (Noguchi et al. 1993; Ye et al. 2008). We saw no evidence of age-related effects in our CASA data or morphological examination of spermatozoa in these mice (Fig. 1 and 2). This suggests that the developmental defects in the *Cstf2t*$^{-/-}$ mice are consistent throughout the period we measured.

We also hypothesized that lack of *Cstf2t* might result in changes in numbers of resident somatic cells in testes, possibly due to interactions with the affected germ cells. We did not observe this (except for the slight overdominance effect seen in the number of Sertoli cells, Fig. 3C). This finding is not surprising, since τCstF-64 is expressed only in germ cells and not testicular somatic cells. More surprising was the finding that numbers of round spermatids were affected in *Cstf2t*$^{-/-}$ mice, but not numbers of spermatogonia, primary spermatocytes, or secondary spermatocytes (Fig. 3D). Expression of τCstF-64 in germ cells begins in pachynema and continues until elongating spermatids (Wallace et al. 1999), and the earliest visible lesions in the *Cstf2t*$^{-/-}$ mice were secondary spermatocytes (Dass et al. 2007). This suggested that we might expect differences in primary and secondary spermatocytes, which we did not observe (Fig. 3D). Our new data lead us to conclude that the primary role of τCstF-64 is postmeiotic, or that genes that are affected by τCstF-64 during meiosis delay their expression until after meiosis, or that effects on a critical number genes are required for a phenotypic change that is microscopically visible. Future experiments will test these possibilities.

Plasma testosterone and testicular LH-stimulated testosterone secretion in vitro appeared to be reduced in *Cstf2t*$^{-/-}$ mice (Fig. 5). Spermatogenesis takes place in the seminiferous tubules of the testis, where testosterone and FSH are accepted as the two major hormones that are crucial for this process. Stereological estimates showed that the seminiferous tubule volume per testis was lower in KO mice than in WT or HET mice (Fig. 4), suggesting that KO mice have less capacity to produce sperm compared to WT and HET mice. Interestingly, although Leydig cell numbers (Fig. 3C) and volume (Fig. 4) in KO mice were similar to those of WT and HET mice, it appeared that these cells were not secreting as much testosterone as Leydig cells in WT and HET mice (Fig. 5). Our previous studies (Dass et al. 2007; Tardif et al. 2010) had led us to conclude that the majority of the defects in spermiogenesis were due solely to reduced expression of key genes within the germ cells population. This is our first hint that loss of τCstF-64 affects non-germ cells in the *Cstf2t*$^{-/-}$ mice; possibly Leydig cells are responding to reduced numbers of postmeiotic germ cells. These new data further suggest the alternate hypothesis that reduced androgen contributes to the spermiogenic deficiencies in *Cstf2t*$^{-/-}$ mice.

Because there was considerable precedent for a role of CstF-64 in control of immune cell function and immunoglobulin switching (Martincic et al. 2009; Martincic et al. 1998; Shell et al. 2005; Takagaki and Manley 1998; Takagaki et al. 1996), we hypothesized that τCstF-64 might play a similar role. For example, if τCstF-64 were responsible for the switch

from the membrane-bound to the secreted form of IgG, a possible consequence of loss of τCstF-64 would be a reduction in plasma IgG, and possibly a block to B cell maturation. We found that, like CstF-64, τCstF-64 was in complex with CstF-50 in immune cell lines and splenocytes (Fig. 6C). This would be necessary if τCstF-64 were to control immunoglobulin mRNA polyadenylation. However, we saw no significant difference in the amounts of IgG or IgM in *Cstf2t*$^{-/-}$ mice than in wild type mice, eliminating that possibility. Another hypothesis was that τCstF-64 was important for the differentiation of one or more immune cell types. However, we saw no detectable differences in numbers of splenocytes or bone marrow cells or in cells exhibiting different immune cell markers (Supplemental Table 1), so that hypothesis was not supported.

We did see an increase in τCstF-64 in LPS-stimulated CD19^{+} B cells (Fig. 6B). However, since this increase was parallel to the increase shown by CstF-64 in the same cells, we can only conclude that τCstF-64 responds to the same signals as does CstF-64. Therefore, while it is expressed in immune cells, we conclude that τCstF-64 is not critical for B cell development or other normal immune functions. We have not eliminated the possibility that physiologically specialized functions might require τCstF-64, however. These results came as a surprise: why should τCstF-64 expression in germ cells be essential for their development, but expression in immune cells or neural cells not be essential for theirs? The most parsimonious argument we can make is that, because τCstF-64 exists for a necessary germ cell function, other tissues have taken advantage of it to increase their options for diversity of gene expression, but have developed no stringent necessity. Perhaps with more subtle tests than we have devised here, we might find that τCstF-64 participates in a physiological response in these tissues, but so far, we have no evidence for that possibility.

5. Conclusion

We showed here that τCstF-64 is part of the CstF complex in immune cells (Fig. 6C); and have similar evidence in testis (data not shown). These data argue for the likelihood that the germ cell defects in *Cstf2t*$^{-/-}$ mice are due to incorrect polyadenylation of critical germ cell mRNAs, and not to a cryptic non-polyadenylation function of τCstF-64. In other experiments not discussed here, we have been examining genes that are affected directly by τCstF-64. One of our preliminary findings is that polyadenylation of these mRNAs is reduced but not eliminated. This suggests that, even in male germ cells where τCstF-64's in fluence is greatest, other mechanisms compensate at least partially for its absence. Our future experiments will look toward tying together these different mechanisms to better understand polyadenylation control of tissue-specific gene expression.

Supplementary Material

Refer to Web version on PubMed Central for supplementary material.

Abbreviations

ANOVA	analysis of variance
CstF	cleavage stimulation factor
CASA	computer-assisted sperm analysis
dpp	days postpartum
LPS	lipopolysaccharide
LH	luteinizing hormone

MFI	mean fluorescent intensity
MSCI	meiotic sex chromosome inactivation

Acknowledgments

We wish to thank Steve Tardif and Kim Chau for help in the CASA experiments, James Hutson, Charles Faust, and Stephen White for advice on data analysis, Jeffrey Thomas for discussions on terminology, Julianne L. Baron for help with statistical analyses, and Andrew Hockert for comments on the manuscript.

References

Ariyaratne HB, Mendis-Handagama SMLC. Changes in the testis interstitium of Sprague Dawley rats from birth to sexual maturity. Biol Reprod. 2000; 62(3):680–690. [PubMed: 10684810]

Beyer K, Dandekar T, Keller W. RNA ligands selected by cleavage stimulation factor contain distinct sequence motifs that function as downstream elements in 3′-end processing of pre-mRNA. Journal of Biological Chemistry. 1997; 272(42):26769–26779. [PubMed: 9334264]

Bhasin S, Mallidis C, Ma K. The genetic basis of infertility in men. Baillière's Best Practice & Research Clinical Endocrinology & Metabolism. 2000; 14(3):363–388.

Buratowski S. Connections between mRNA 3′ end processing and transcription termination. Current Opinions in Cell Biology. 2005; 17(3):257–261.

Dass B, McDaniel L, Schultz RA, Attaya E, MacDonald CC. The gene CSTF2T encoding the human variant CstF-64 polyadenylation protein τCstF-64 is intronless and may be associated with male sterility. Genomics. 2002; 80:509–514. [PubMed: 12408968]

Dass B, McMahon KW, Jenkins NA, Gilbert DJ, Copeland NG, MacDonald CC. The gene for a variant form of the polyadenylation protein CstF-64 is on chromosome 19 and is expressed in pachytene spermatocytes in mice. Journal of Biological Chemistry. 2001; 276(11):8044–8050. [PubMed: 11113135]

Dass B, Tardif S, Park JY, Tian B, Weitlauf HM, Hess RA, Carnes K, Griswold MD, Small CL, MacDonald CC. Loss of polyadenylation protein τCstF-64 causes spermatogenic defects and male infertility. Proceedings of the National Academy of Science, USA. 2007; 104(51):20374–20379.

Edwalds-Gilbert G, Milcarek C. Regulation of poly(A) site use during mouse B-cell development involves a change in the binding of a general polyadenylation factor in a B-cell stage-specific manner. Molecular and Cellular Biology. 1995; 15(11):6420–6429. [PubMed: 7565794]

Grootegoed JA, Siep M, Baarends WM. Molecular and cellular mechanisms in spermatogenesis. Baillière's Best Practice & Research Clinical Endocrinology & Metabolism. 2000; 14(3):331–343.

Handel MA. The XY body: a specialized meiotic chromatin domain. Experimental Cell Research. 2004; 296(1):57–63. [PubMed: 15120994]

Hirsh A. Male subfertility. BMJ. 2003; 327(7416):669–672. [PubMed: 14500443]

Huber Z, Monarez RR, Dass B, MacDonald CC. The mRNA encoding τCstF-64 is expressed ubiquitously in mouse tissues. Annals of the New York Academy of Sciences. 2005; 1061:163–172. [PubMed: 16467265]

Isidori A, Latini M, Romanelli F. Treatment of male infertility. Contraception. 2005; 72(4):314–318. [PubMed: 16181978]

Keene JD. Minireview: global regulation and dynamics of ribonucleic acid. Endocrinology. 2010; 151(4):1391–1397. [PubMed: 20332203]

Khil PP, Smirnova NA, Romanienko PJ, Camerini-Otero RD. The mouse X chromosome is enriched for sex-biased genes not subject to selection by meiotic sex chromosome inactivation. Nat Genet. 2004; 36(6):642–646. [PubMed: 15156144]

Licatalosi DD, Darnell RB. RNA processing and its regulation : global insights into biological networks. Nat Rev Genet. 2010; 11(1):75–87. [PubMed: 20019688]

Liu D, Brockman JM, Dass B, Hutchins LN, Singh P, McCarrey JR, MacDonald CC, Graber JH. Systematic variation in mRNA 3′-processing signals during mouse spermatogenesis. Nucleic Acids Research. 2007; 35:234–246. [PubMed: 17158511]

Lutz CS. Alternative polyadenylation: a twist on mRNA 3′ end formation. ACS Chem Biol. 2008; 3(10):609–617. [PubMed: 18817380]

MacDonald CC, McMahon KW. Tissue-Specific Mechanisms of Alternative Polyadenylation: Testis, Brain and Beyond. WIRES-RNA. 2010 In the press.

Martincic K, Alkan SA, Cheatle A, Borghesi L, Milcarek C. Transcription elongation factor ELL2 directs immunoglobulin secretion in plasma cells by stimulating altered RNA processing. Nat Immunol. 2009; 10(10):1102–1109. [PubMed: 19749764]

Martincic K, Campbell R, Edwalds-Gilbert G, Souan L, Lotze MT, Milcarek C. Increase in the 64-kDa subunit of the polyadenylation/cleavage stimulatory factor during the G0 to S phase transition. Proceedings of the National Academy of Science, USA. 1998; 95(19):11095–11100.

Mendis-Handagama SMLC, Ariyaratne HB, Fecteau KA, Grizzle JM, Jayasundera NK. Comparison of testis structure, function and thyroid hormone levels in control C57BL/6 mice and anti-mullerian hormone over expressing mice. Histol Histopathol. 2010; 25(7):901–908. [PubMed: 20503178]

Mendis-Handagama SMLC, Ariyaratne HB, Teunissen van Manen KR, Haupt RL. Differentiation of adult Leydig cells in the neonatal rat testis is arrested by hypothyroidism. Biol Reprod. 1998; 59(2):351–357. [PubMed: 9687307]

Mendis-Handagama SMLC, Ewing LL. Sources of error in the estimation of Leydig cell numbers in control and atrophied mammalian testes. J Microsc. 1990; 159(Pt 1):73–82. [PubMed: 2204704]

Mendis-Handagama SMLC, Kerr JB, de Kretser DM. Experimental cryptorchidism in the adult mouse: I. Qualitative and quantitative light microscopic morphology. J Androl. 1990; 11(6):539–547. [PubMed: 1982285]

Mendis-Handagama SMLC, Zirkin BR, Ewing LL. Comparison of components of the testis interstitium with testosterone secretion in hamster, rat, and guinea pig testes perfused in vitro. Am J Anat. 1988; 181(1):12–22. [PubMed: 3348144]

Moore MJ, Proudfoot NJ. Pre-mRNA processing reaches back to transcription and ahead to translation. Cell. 2009; 136(4):688–700. [PubMed: 19239889]

Noguchi J, Yoshida M, Ikadai H, Imamichi T, Watanabe G, Taya K. Age-related changes in blood concentrations of FSH, LH and testosterone and testicular morphology in a new rat sterile mutant with hereditary aspermia. J Reprod Fertil. 1993; 97(2):433–439. [PubMed: 8501713]

Parsons PA, Bodmer WF. The evolution of overdominance: natural selection and heterozygote advantage. Nature. 1961; 190:7–12. [PubMed: 13733020]

Quill TA, Sugden SA, Rossi KL, Doolittle LK, Hammer RE, Garbers DL. Hyperactivated sperm motility driven by CatSper2 is required for fertilization. Proceedings of the National Academy of Science, USA. 2003; 100(25):14869–14874.

Shell SA, Hesse C, Morris SM Jr, Milcarek C. Elevated levels of the 64-kDa cleavage stimulatory factor (CstF-64) in lipopolysaccharide-stimulated macrophages influence gene expression and induce alternative poly(A) site selection. Journal of Biological Chemistry. 2005; 280(48):39950–39961. [PubMed: 16207706]

Sterio DC. The unbiased estimation of number and sizes of arbitrary particles using the disector. J Microsc. 1984; 134(Pt 2):127–136. [PubMed: 6737468]

Takagaki Y, Manley JL. Levels of polyadenylation factor CstF-64 control IgM heavy chain mRNA accumulation and other events associated with B cell differentiation. Molecular Cell. 1998; 2:761–771. [PubMed: 9885564]

Takagaki Y, Manley JL, MacDonald CC, Wilusz J, Shenk T. A multisubunit factor CstF is required for polyadenylation of mammalian pre-mRNAs. Genes & Development. 1990; 4:2112–2120. [PubMed: 1980119]

Takagaki Y, Seipelt RL, Peterson ML, Manley JL. The polyadenylation factor CstF-64 regulates alternative processing of IgM heavy chain pre-mRNA during B cell differentiation. Cell. 1996; 87:941–952. [PubMed: 8945520]

Tardif S, Akrofi A, Dass B, Hardy DM, MacDonald CC. Infertility with impaired zona pellucida adhesion of spermatozoa from mice lacking τCstF-64. Biol Reprod. 2010; 83(3):464–472. [PubMed: 20463354]

Turner JM. Meiotic sex chromosome inactivation. Development. 2007; 134(10):1823–1831. [PubMed: 17329371]

Verstegen J, Iguer-Ouada M, Onclin K. Computer assisted semen analyzers in andrology research and veterinary practice. Theriogenology. 2002; 57(1):149–179. [PubMed: 11775967]

Wallace AM, Dass B, Ravnik SE, Tonk V, Jenkins NA, Gilbert DJ, Copeland NG, MacDonald CC. Two distinct forms of the 64,000 Mr protein of the cleavage stimulation factor are expressed in mouse male germ cells. Proceedings of the National Academy of Science, USA. 1999; 96(12): 6763–6768.

Wallace AM, Denison T, Attaya EN, MacDonald CC. Developmental differences in expression of two forms of the CstF-64 polyadenylation protein in rat and mouse. Biology of Reproduction. 2004; 70(4):1080–1087. [PubMed: 14681198]

Wang PJ. X chromosomes, retrogenes and their role in male reproduction. Trends in Endocrinology and Metabolism. 2004; 15(2):79–83. [PubMed: 15036254]

Ye X, Skinner MK, Kennedy G, Chun J. Age-dependent loss of sperm production in mice via impaired lysophosphatidic acid signaling. Biol Reprod. 2008; 79(2):328–336. [PubMed: 18448840]

Zamudio NM, Chong S, O'Bryan MK. Epigenetic regulation in male germ cells. Reproduction. 2008; 136(2):131–146. [PubMed: 18515312]

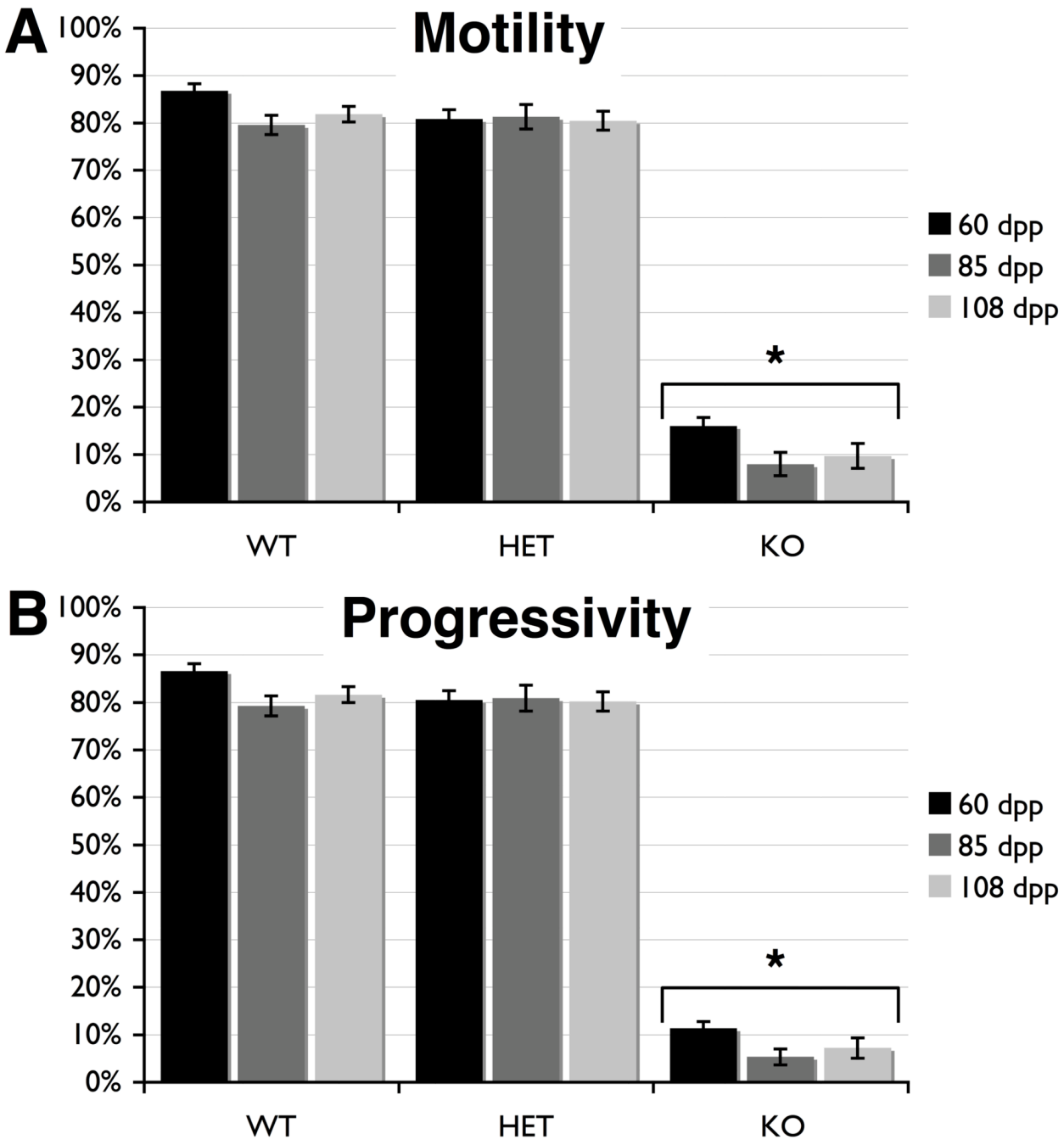

Fig. 1.

Computer-assisted sperm analysis (CASA) shows that spermatozoa from *Cstf2t*$^{-/-}$ mice have severe motility defects in mice of all ages. CASA was performed on cauda epididymal contents of mice at 60 (black bars), 85 (dark gray bars) and 108 dpp (light gray bars) that were wild type (WT), *Cstf2t*$^{+/-}$ (HET), or *Cstf2t*$^{-/-}$ (KO). **A**) Numbers of motile spermatozoa are indicated as a percent of the total. **B**) Numbers of motile spermatozoa that displayed progressive linear movement with a speed higher than 25 μm/sec as a percent of the total. Error bars are standard errors of the mean; asterisks indicate groups that were significantly different from other groups ($P < 0.001$) after ANOVA using Kruskal-Wallis

non-parametric method and Dunn's multiple comparisons post-test. Other CASA parameters are listed in Supplemental Table 1.

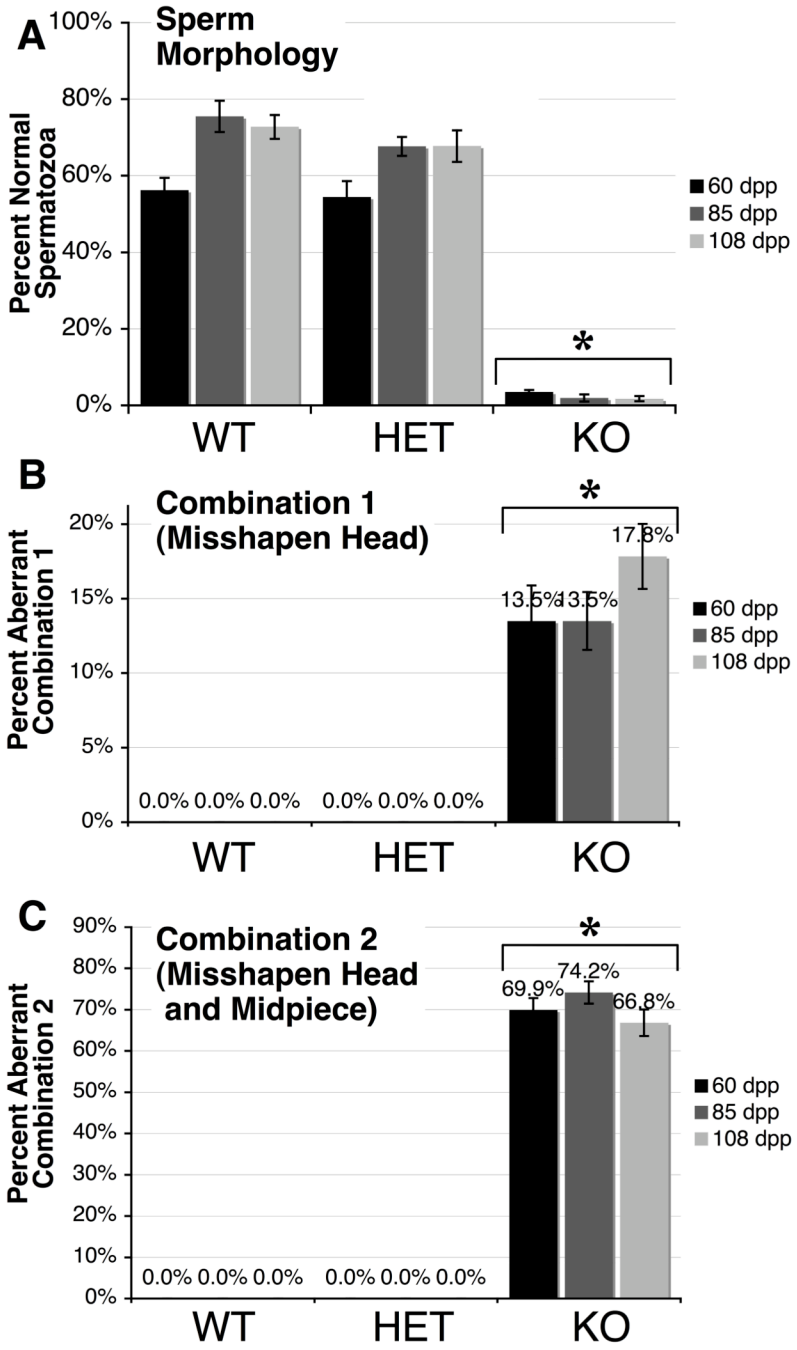

Fig. 2.

Sperm morphology of *Cstf2t*$^{-/-}$ mice is greatly abnormal. Sperm smears from mouse cauda were examined and scored as “normal” (lacking visible defects) or as displaying head, midpiece or tail anomalies (see Materials and Methods). Scoring was performed on caudal smears from mice at 60 (black bars), 85 (dark gray bars) and 108 dpp (light gray bars) that were wild type (WT), *Cstf2t*$^{+/-}$ (HET), or *Cstf2t*$^{-/-}$ (KO). **A**) Percent of spermatozoa that appeared normal. **B**) Percent of spermatozoa that had misshapen and variably microcephalous heads (Combination 1). **C**) Percent of spermatozoa that had misshapen, variably microcephalous heads, and thin or indistinguishable midpieces (Combination 2). Error bars are standard errors of the mean; asterisks indicate groups that were significantly

different from other groups ($P < 0.001$) after ANOVA using Kruskal-Wallis non-parametric method and Dunn's multiple comparisons post-test. Other morphology scores are listed in Supplemental Table 2.

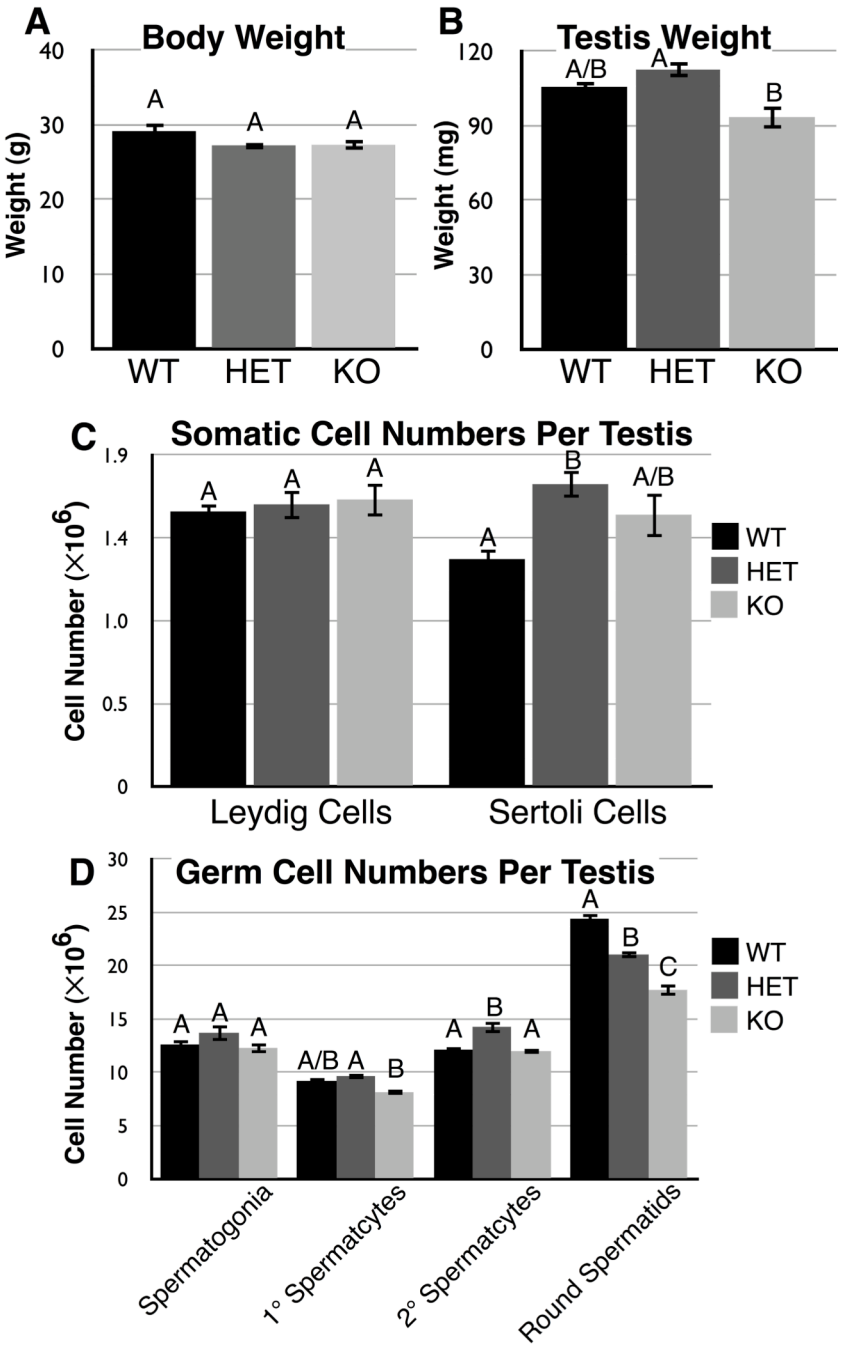

Fig. 3.

Body weights, testis weights, and numbers of testis-resident somatic cells of *Cstf2t*$^{-/-}$ mice do not differ from wild type mice, but numbers of round spermatids are significantly diminished. Male mice ranging in age from 88 to 136 dpp were used in this study. **A**) Body weights (in grams) of wild type (WT, black bars), *Cstf2t*$^{+/-}$ (HET, dark gray bars) and *Cstf2t*$^{-/-}$ (KO, light gray bars) mice (not significant). **B**) Testis weights (in milligrams) of wild type, *Cstf2t*$^{+/-}$ and *CSTF2T*$^{-/-}$ mice (P = 0.0028). **C**) Numbers of resident somatic cells per testis. Left, number of Leydig cells (not significant); right, number of Sertoli cells (P = 0.0193). **D**) Numbers of germ cells per testis. From left to right: spermatogonia (not significant), primary spermatocytes (P = 0.0167), secondary spermatocytes (P = 0.0007),

and round spermatids ($P < 0.0001$). Values with the same letter indicate measurements that were not significantly different after ANOVA and a Tukey post-test.

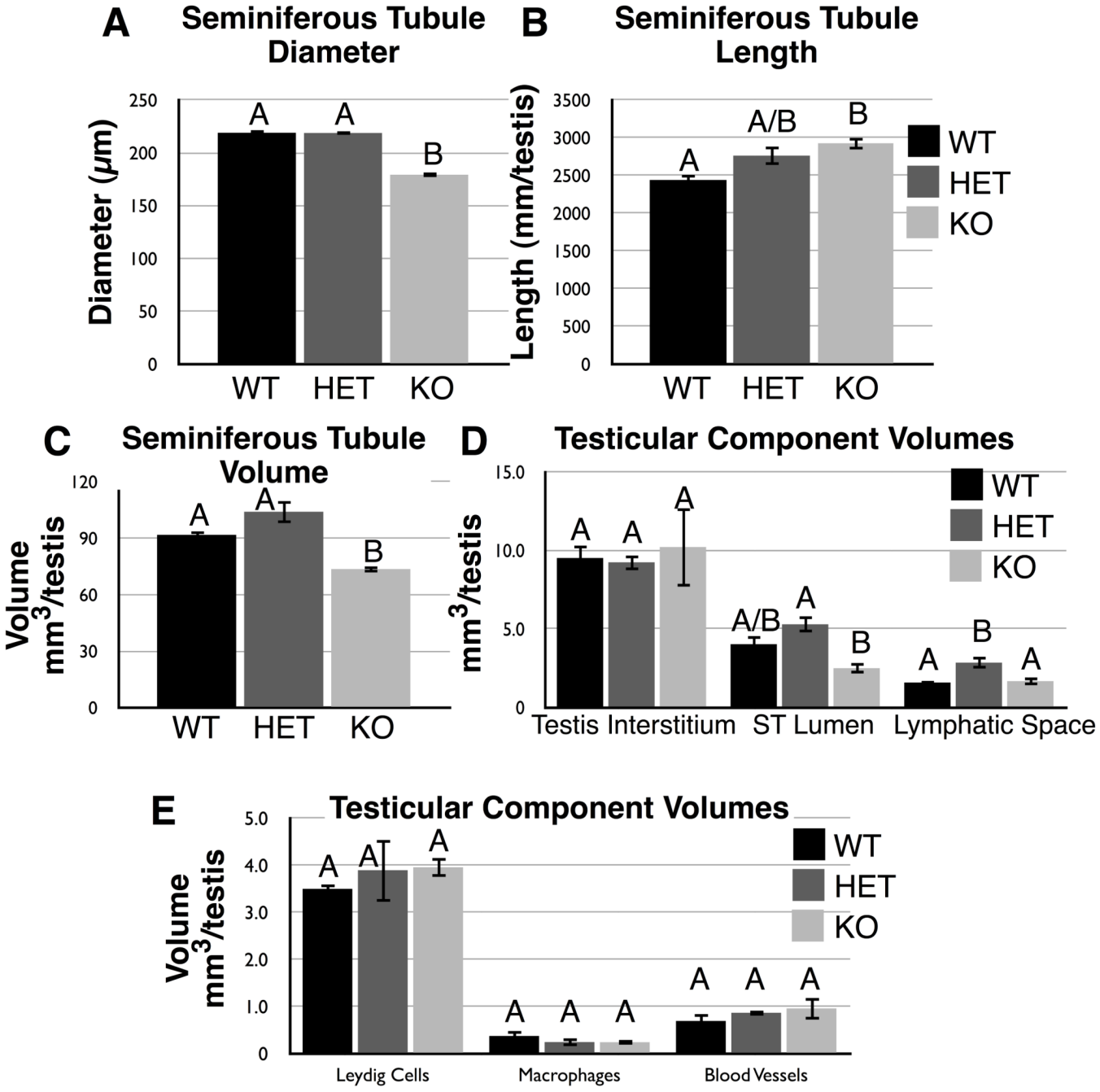

Fig. 4.

Stereological measurements of testicular components from wild type (WT), *Cstf2t*$^{+/-}$ (HET), or *Cstf2t*$^{-/-}$ (KO) mice. See Materials and Methods for description of each parameter. **A**) Seminiferous tubule diameter. **B**) Seminiferous tubule length. **C**) Seminiferous tubule volume. **D**) Volumes of other testicular components. **E**) Volumes of other testicular cell types.

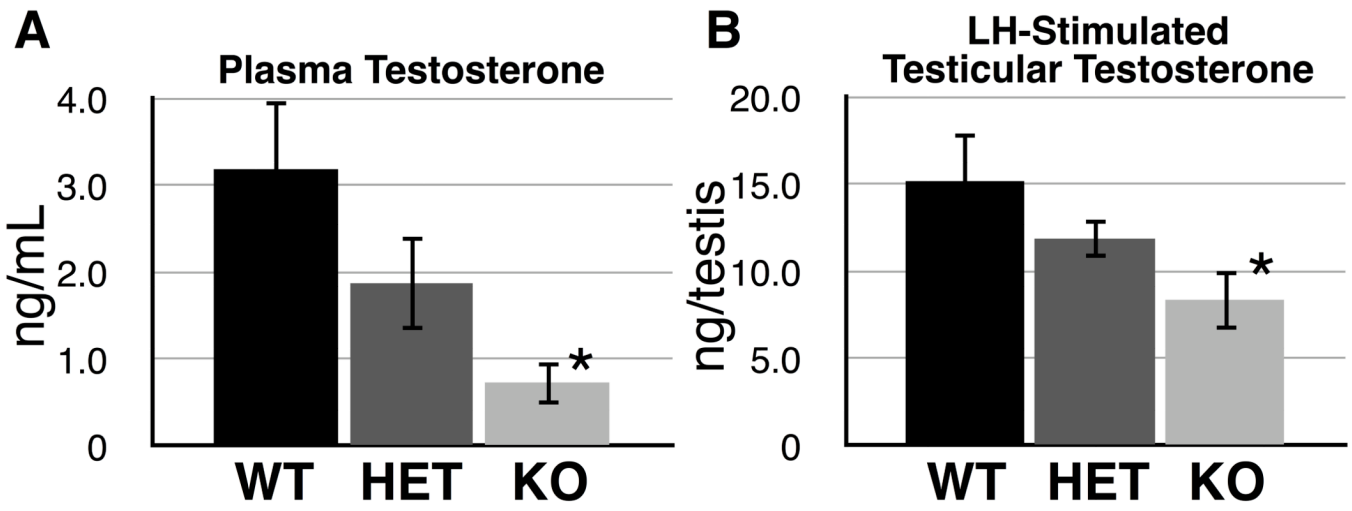

Fig. 5.

Plasma testosterone is diminished in male *Cstf2t*$^{-/-}$ mice. **A**) Testosterone was measured by RIA from cardiac blood taken at the time of death from wild type (WT), *Cstf2t*$^{+/-}$ (HET), or *Cstf2t*$^{-/-}$ (KO) male mice. Error bars are standard errors of the mean; the asterisk represents a sample (KO) that was significantly different than the wild type (P = 0.0245) by ANOVA. **B**) Decapsulated testes were treated with LH (Materials and Methods); RIA-measured testosterone was determined for the entire testis. Error bars are standard errors of the mean; the asterisk represents a sample (KO) that was significantly different from wild type (P < 0.05) by ANOVA.

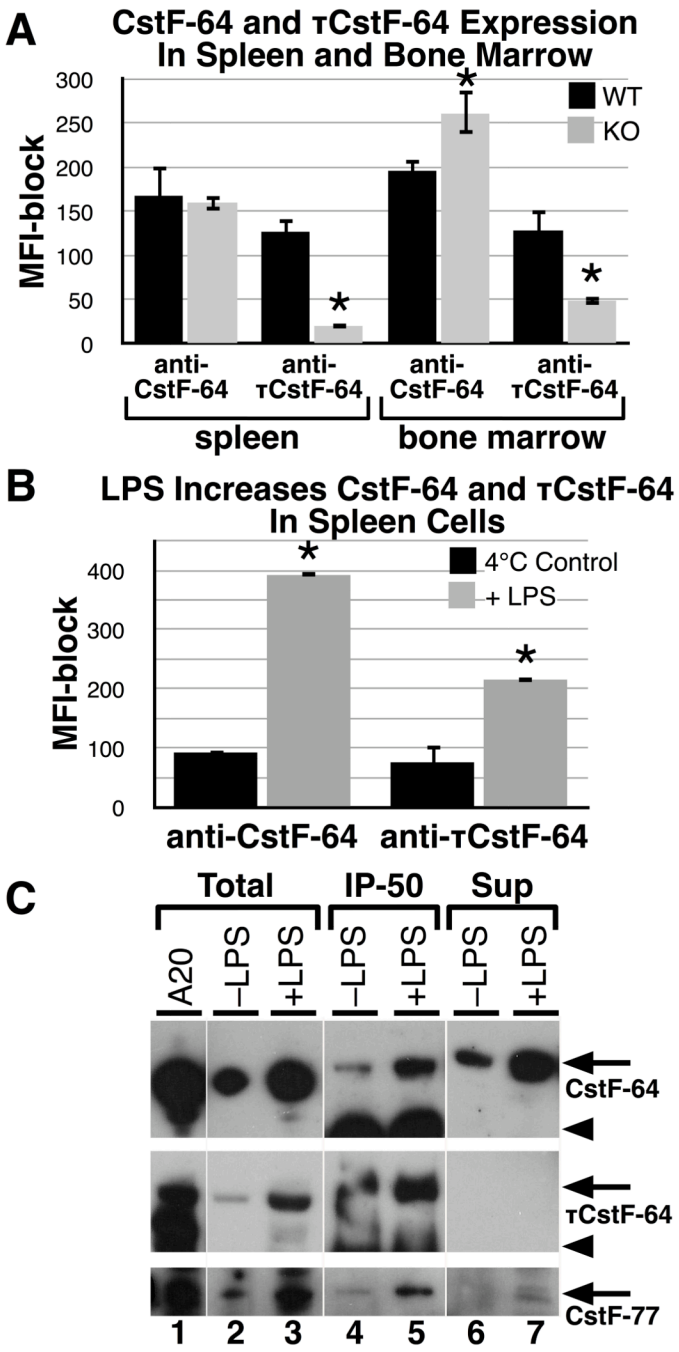

Fig. 6.

CstF-64 and τCstF-64 are both expressed in lymphoid cells where they interact with CstF-50 and CstF-77. Mean fluorescent intensities (MFI) of CstF-64 (3A7 antibody) versus τCstF-64 (6A9 antibody) in spleen and bone marrow cells from three wild type and three *Cstf2t*$^{-/-}$ mice were determined. Cells were isolated and stained for intracellular proteins with fluorescently tagged (FITC) 3A7 or 6A9 monoclonal antibodies. Parallel samples were blocked with an excess of the identical unlabelled monoclonal antibody. The MFI-block values are plotted on the Y-axes. Error bars represent the standard error of the mean (S.E.M.) from at least three mice of each type. Asterisks represent values that significantly differ ($P < 0.05$) from the paired samples, using the Student's t test. **A**) Total freshly isolated

spleen cells and cells flushed from bone marrow from male wild type (WT) and *Cstf2t*$^{-/-}$ (KO) mice were stained and analyzed for CstF-64 (anti-CstF-64) or τCstF-64 (anti-τCstF-64) expression. MFI values less the unlabelled antibody-blocked MFI values are shown. **B**) CD19^{+} B cells from spleen were isolated and incubated either at 4°C or stimulated with lipopolysaccharide (LPS) for 72 hours. Relative CstF-64 or τCstF-64 MFI values were determined. **C**) Aliquots of lysed splenic B cells treated as in panel B were run on SDS-10%PAGE (whole cells, WC) or immunoprecipitated with anti-CstF-50 antibody prior to SDS-PAGE (IP50) to isolate the CstF complexes. CstF-77 was detected using the rabbit anti-CstF-77 antibody (Materials and Methods). A20 cell extract was run as a size control. Arrows indicate the mobilities of CstF-64, τCstF-64, or CstF-77, as indicated; arrowheads indicate the mobility of mouse IgG in the IP-50 lanes (lanes 4 and 5).

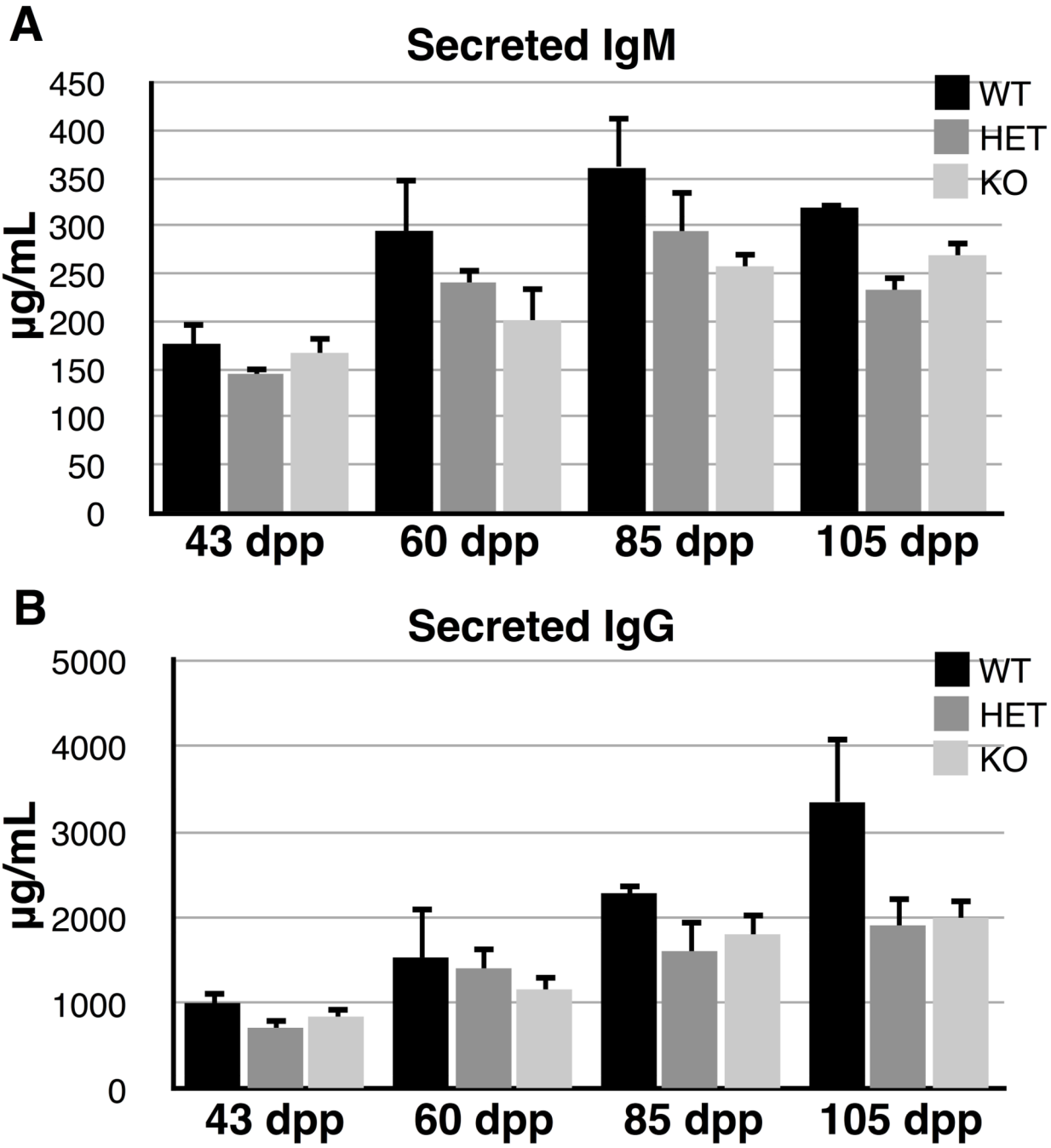

Fig. 7.

Cstf2t$^{+/+}$ (wild type, WT) versus the *Cstf2t*$^{+/-}$ (HET) or *Cstf2t*$^{-/-}$ (KO) IgG serum levels. IgM and IgG levels in the blood were determined by ELISA. Each bar represents levels from at least three mice of the indicated ages. The data were analyzed by a two-way ANOVA using Tukey's HSD post test. Error bars represent standard error of the mean (S.E.M.). The F value was 6.06. **A**) IgM levels. **B**) IgG levels.

Table 1

Percentage of bone marrow cells positive for specific cell surface markers

	bone marrow			spleen		
	WT	KO	S.E.	WT	KO	S.E.
Gr-1	44.67		1.45	4.10		1.56
		48.67	1.67		6.00	1.44
CD11b	46.97		1.73	8.10		1.02
		48.18	1.90		8.11	1.42
CD19	32.37		6.82	44.33		3.06
		32.50	7.59		45.50	0.87
IgM	6.26		1.66	22.47		5.10
		5.67	2.10		20.20	1.80
Syndecan	48.96		8.14	42.01		2.19
		48.40	8.32		45.09	1.11
NK1.1	1.31		0.16	9.21		5.32
		1.12	0.06		10.79	4.27
B220	29.30		3.82	45.00		7.82
		24.67	4.84		46.27	5.85
CD3	14.54		3.30	33.67		5.17
		14.94	3.10		34.50	5.35